Langmuir

Article

pubs.acs.org/Langmuir

Synthesis and Characterization of Colloidal Fluorescent Silver Nanoclusters

Sherry Huang,[†,‡,§,∥] Christian Pfeiffer,[‡,∥] Jana Hollmann,[‡] Sebastian Friede,[‡] Justin Jin-Ching Chen,[§] Andreas Beyer,[‡] Benedikt Haas,[‡] Kerstin Volz,[‡] Wolfram Heimbrodt,[‡] Jose Maria Montenegro Martos,*[,‡] Walter Chang,[§] and Wolfgang J. Parak*[,‡]

[†]Institute of Polymer Science and Engineering, National Taiwan University, Taipei, Taiwan

[‡]Fachbereich Physik and WZMW, Philipps Universität Marburg, Marburg, Germany

[§]Department of Biomedical Engineering, Chung Yuan Christian University, Chungli, Taiwan

Supporting Information

ABSTRACT: Ultrasmall water-soluble silver nanoclusters are synthesized, and their properties are investigated. The silver nanoclusters have high colloidal stability and show fluorescence in the red. This demonstrates that like gold nanoclusters also silver nanoclusters can be fluorescent.

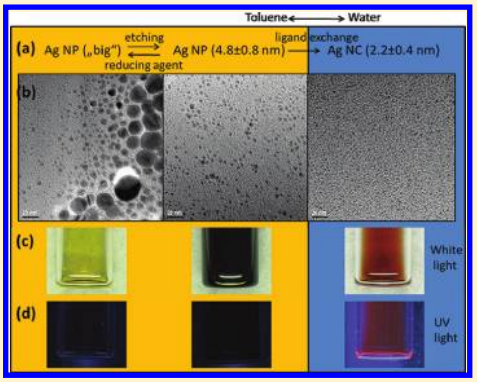

INTRODUCTION

Recently, it has been demonstrated by a variety of groups that gold nanoclusters (NCs) are fluorescent.[1−7] Though colloidal gold nanoparticles (NPs) have been in use over decades of time,[8,9] this feature has been only popularized recently. While fluorescence of bigger gold NPs (bigger than ≈5 nm) is at maximum very low, smaller gold NPs (smaller than ≈3 nm), which are also often termed as gold NCs, show a remarkable fluorescence with quantum yields (QY) up to a few percent (diameter, QY: 2 nm, 3.5%; ≤1 nm, 5%; ≤1 nm, 3.7%;[10] 0.92 nm, 0.07%;[11] 2 nm, 2%;[12] 1.4 nm, 0.6%;[13] 1.8 nm, 8%.[14]) This fact is interesting in two directions. First, the possibility of having well-defined Au NCs allows for detailed investigation of their photophysical properties and thus it is an interesting model system for investigating size-dependent optical properties of materials. In this way, besides colloidal quantum dots,[15−19] also Au NCs show size-dependent fluorescence, that is, effects on downscaling materials from bulk to nanometer dimensions, though the photophysical mechanisms are different. Second, due to their small size, Au NCs are potentially useful for labeling of biological structures.[2,5,11,12] Compared to semiconductor NPs (quantum dots), their lower quantum yield is compensated by the fact that they do not contain any intrinsically toxic material, as, for example, cadmium. Thus, Au NCs could be used for labeling of small biological structures which they are still able to penetrate, such as, for example, the synaptic cleft.

Though in the last years several reports have been published around fluorescent Au NCs, studies for similar Ag NCs are still scarce.[20−31] Silver is another noble metal, which similar to gold exhibits plasmonic properties on the nanometer scale. Next to Au NPs, Ag NPs are the most studied system of colloidal metal NPs. Initially, interest in Au NPs mainly arose from their high electron density, which has been used for immunostaining with Au NPs as marker for transmission electron based imaging.[32] Later on, the plasmonic properties of Au NPs have been widely used for colorimetric detection of biological molecules.[33,34] In contrast, Ag NPs have been initially considered because of their antibacterial activity.[35−42] Different pathways about the cytotoxicity of Ag NPs have been observed.[43−46] It is generally believed that release of Ag^+ from the Ag NPs surface upon corrosion[47] is a major source for cytotoxicity, though it is still under discussion if Ag NPs are more or less toxic compared to an equivalent amount of Ag^+ ions.[45,48]

Similarity between Au and Ag NPs motivated us to transfer a recent synthetic route for fluorescent Au NCs[2] to produce Ag NCs. The synthetic approaches to obtain Ag NCs previously reported follow two major synthetic routes.[49] The stabilization of the Ag NCs can be made using polymers or dendrimers as

Special Issue: Colloidal Nanoplasmonics

Received: January 31, 2012
Revised: March 22, 2012
Published: March 26, 2012

ligand and/or scaffold,[50] using DNA/oligonucleotides,[51] or proteins[24] for stabilization. Methods using an inorganic scaffold such as zeolites[52,53] have also been reported. The Ag NCs in the current report are not stabilized by one of these methods, but by using small organic molecules. This methodology is scarcely present in the literature,[26] but has the advantage that the Ag NCs are separated because of their electrostatic repulsion. However, the use of small molecules for stabilization usually leads to weaker fluorescence emission in comparison with other molecules such as proteins. All the synthetic methods start from an Ag^+ precursor that must be reduced to Ag^0. This reduction can be done chemically,[23,24,26] or by visible light,[22] UV-light,[54,55] microwaves,[25] or sonochemically.[56] The reduction of the Ag NCs synthesized in this work is done chemically, but by changing the commonly used sodium borohydride ($NaBH_4$) for tetrabutylammonium borohydride (TBAB), which is not such a strong reducing agent such as $NaBH_4$.

Thus, in this work, we want to demonstrate an easy synthesis route for colloidally stable Ag NCs in aqueous solutions. These NCs are fluorescent, though their quantum yield is arguably relatively small.

RESULTS AND DISCUSSION

Recently, a protocol for the synthesis of fluorescent Au NCs has been published by our research group.[2] The same synthetic strategy can be also applied for making Ag NCs. Synthesis started with the reduction of a Ag^+ precursor (AgCl) complexed by didodecyldimethylammonium bromide and decanoic acid, dissolved in toluene to Ag^0 by addition of tetrabutylammonium borohydride as reducing agent. Reduction leads to the formation of Ag NPs capped with didodecyldimethylammonium bromide and decanoic acid dissolved in toluene.[57] These Ag NPs displayed the typical surface plasmon peak around 430 nm. The inorganic Ag core diameters (i.e., the NP diameters without organic ligand capping) had a broad size distribution as determined by transmission electron microscopy (TEM), though many NPs had diameters around 4 nm (cf. Figure 1 and the Supporting Information). The size distribution was improved by further dropwise addition of Ag^+ precursor solution. Hereby, the bigger NPs were etched to smaller sizes. Narrowing of the size distribution was monitored by the increased intensity of the surface plasmon peak (cf. Supporting Information), which finally led to a mean Ag NP diameter of 4.8 ± 0.8 nm. In a subsequent step, phase transfer to aqueous solution was performed. The Ag NPs dissolved in toluene were precipitated by the addition of freshly prepared lipoic acid and didodecyldimethylammonium bromide, followed by heating and UV-light exposure. Following several purification steps, the precipitate was dissolved in aqueous solution (SBB9, 50 mM sodium borate buffer, pH 9). The phase transfer step led to two important changes. First, the size of the Au NPs was further decreased, leading to Ag NCs with an average Ag core diameter (as determined with TEM) of 2.2 ± 0.4 nm (cf. Figure 1 and the Supporting Information). High-resolution TEM (HR-TEM) using fast Fourier transform (FFT) experiments was carried out (cf. Figure 2). In the FFT image, one can observe two distinct rings which can be attributed to two main diffracting planes, the {111} and the {002} planes of Ag, which theoretically appear at 4.319 and 4.988 nm^{-1} respectively. The theoretical position of the Ag diffraction is indicated as red half rings. Possible byproducts such as silver chloride (AgCl) and silver oxide (Ag_2O) do not show any diffraction in this range;

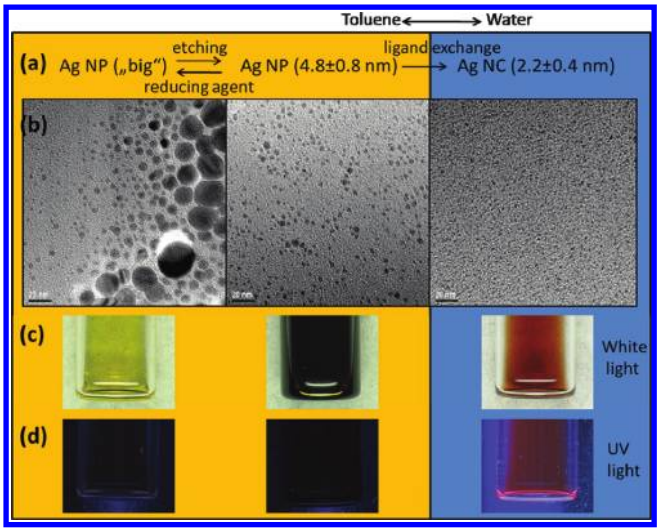

Figure 1. (a) General procedure for the synthesis of Ag nanoclusters (Ag NCs). Big and not well-defined silver nanoparticles (Ag NPs) stabilized by DDAB were etched to well-defined smaller Ag NP by addition of more silver precursor. The hydrophobic Ag NPs were etched to very small hydrophilic Ag NCs upon ligand exchange with dihydrolipoic acid (DHLA). (b) TEM pictures of the three different NPs/NCs. The diameter of the small Ag NPs was determined to be 4.8 ± 0.8 nm and for the Ag NCs 2.2 ± 0.4 nm. The scale bar correspond to 20 nm. (c) Pictures of the different samples under white light illumination. The big Ag NP solution is yellow up to brown in color, the solution of the small Ag NPs is almost black, and the solution of the Ag NCs shows a red-brown color. (d) Pictures of the same solutions under UV light excitation. The Ag NCs show a red fluorescence, whereas the Ag NPs show no fluorescence.

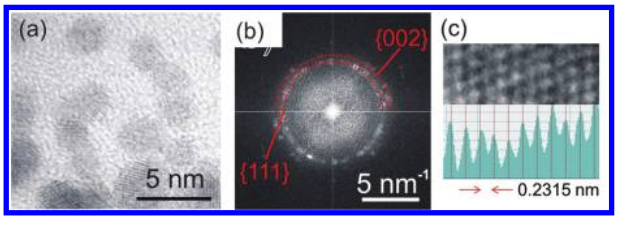

Figure 2. (a) TEM image of several of the Ag nanoclusters. The average diameter of the clusters is between 2 and 3 nm. (b) FFT of the entire image. Two distinct rings can be observed in the FFT, which can be attributed to two main diffracting planes, the {111} and the {002} planes of Ag, which are theoretically at 4.319 and 4.988 nm^{-1}, respectively (red half-rings). (c) High-resolution TEM section of a single NC and corresponding linescan.

hence, it can unambiguously be concluded that the NCs are pure silver. This result is also confirmed examining one single NC, which shows lattice resolution in two directions (cf. Figure 2). The measurement of the lattice spacing from this image shows a regular spacing of planes, with a distance in good agreement with the Ag {111} lattice plane spacing of 0.2315 nm (red dashed lines in the linescan). As well as before, neither AgCl nor Ag_2O has lattice planes in this spacing range, proving the purity of the Ag NCs.[58,59]

The overall hydrodynamic diameter (as determined with dynamic light scattering, cf. the Supporting Information) was 2.7 nm. This demonstrates the presence of lipoic acid on the surface of the Ag NCs, leading to a negative zeta potential of −30 ± 2 mV. Due to this negative charge, the Ag NCs are well dispersed in aqueous solution. Most important, their high colloidal stability allowed for vigorous purification by gel

dx.doi.org/10.1021/la300346t | Langmuir 2012, 28, 8915−8919

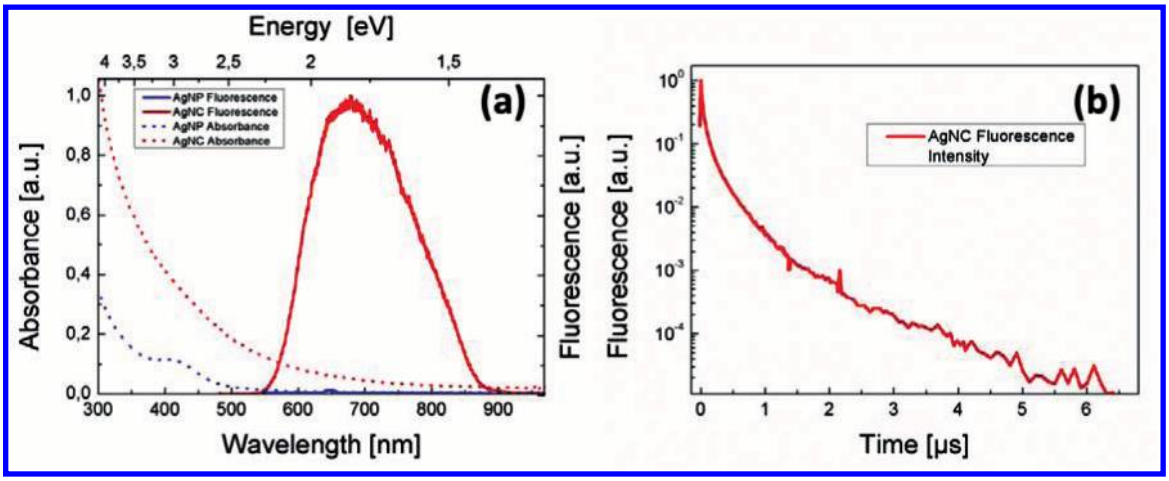

Figure 3. (a) Absorbance (dotted lines) and fluorescence (full lines) spectra of silver nanoparticles (Ag NP) and silver nanoclusters (Ag NC). (b) Transient of the Ag NC fluorescence.

electrophoresis and size exclusion chromatography. These methods warrant for highly purified samples, in which only the Ag NCs but no excess precursors, excess ligands, or intermediated reaction products are present.[60] As second effect, upon phase transfer and capping with lipoic acid, the Ag NCs became fluorescent. It is important to note that fluorescence originating from other compounds in solution but the Ag NCs (such as from not removed precursors) can be excluded due to the vigorous purification.

The fluorescence of the Ag NCs is in the red spectral range, with a broad maximum centered around 680 nm (cf. Figure 3). The quantum yield of the Ag NCs was calculated by the method described by Lakowicz[61] and was determined to be 0.024% (cf. the Supporting Information). Despite this very small value, the fluorescence was clearly above the signal-to-noise-ratio and was even clearly visible by the naked eye. It should be mentioned that, with highly sensitive detectors also for the larger Ag NPs secondary photons, for example, scattered photons can be detected. A comparison is depicted in Figure 3a. It is obvious that the measured intensity of the NCs (which is due to fluorescence) is orders of magnitude stronger. In Figure 3a also the absorption spectra of the NPs and NCs (dotted lines) are depicted. For the NPs, a distinct absorption band can be seen at about 415 nm, which is caused by the surface plasmon of the NPs. This plasmon absorption band is not detectable for the Ag NCs. Such damping of the plasmon absorption with respective weak and broadened absorption is typical for NC sizes around 2 nm.[62,63] Eventually, the question rises from which physical mechanism the fluorescence may occur. It is known that for metal NPs quantum size effects are observable if the diameter is below 2 nm and the NC is made up of just a few atoms.[1,64] For a gold NC of 28 atoms, an intersubband splitting of about 1.7 eV was found.[65] To reveal the physical origin of the red band from the Ag NCs, we performed fluorescence decay measurements. The transient of the red fluorescence is depicted in Figure 3b. The curve exhibits a strong nonexponential decay with decay times in the microsecond range. Such long lifetimes are typical for transitions with rather weak dipole matrix elements. This corresponds well to the fact, that we did not measure a respective absorption band. We therefore conclude that the luminescence is caused by the spatially indirect charge transfer excitons with the electron in the organic shell and the hole in the Ag NC. The conduction band level splitting and shift is obviously large enough to enable a quick transfer of the excited electrons from the NC to the organic shell, namely, the lipoic acid at the surface of the Ag NCs. Only in case of a spatially type II level alignment such electron transfer can compete with intercluster relaxation. It is important to note that Ag NCs and lipoic acid independently and well separated did not show any fluorescence.

It clearly has to be stated that the quantum yield of the Ag NCs is poor. Nevertheless, we performed cellular labeling experiments (cf. Supporting Information). Signal intensity however turned out to be not enough to clearly spatially resolve location of the Ag NCs. Though certainly this indicates that the use of Ag NCs as prepared in this report for fluorescence labeling of cells is limited, in particular due to intrinsic cytotoxicity and low quantum yield, these NCs still provide interesting features. Due to their small hydrodynamic size, they might penetrate in tissue locations where bigger NPs could not enter. They are a complementary material to Au NCs, and in particular to semiconductor NCs, which may help for multiplexed detection. At any rate, due to their high purity and good size distribution, they allow for detailed photophysical characterization, which will help for further understanding of the consequences of downscaling solid state materials on their optical properties. Thus, in case the quantum yield could be improved in the future (such as it has improved for Au NCs upon progressing synthesis protocols), Ag NCs might become applicable for cellular imaging in the future.

■ CONCLUSIONS

We developed ultrasmall water-soluble fluorescent Ag NCs based on a simple wet chemical synthetic route. These Ag NCs possess high colloidal stability and are fluorescent in the red. The Ag NCs are incorporated by cells via nonspecific pathways, and cytotoxic effects are tolerable.

■ SYNTHESIS AND CHARACTERIZATION

The synthesis of Ag NCs has been derived from a previous protocol for the production of fluorescent Au NCs.[2] All the details can be found in the Supporting Information. In brief, first Ag NPs capped with didodecyldimethylammonium bromide (DDAB) were synthesized in toluene and etched down to a size of 4.8 ± 0.8 nm by adding AgCl precursor. During this process, the typical plasmon absorption peak at 430 nm decreased but was still slightly present (see the Supporting

dx.doi.org/10.1021/la300346t | Langmuir 2012, 28, 8915−8919

Information). The peak got lost during the ligand exchange with freshly prepared dihydrolipoic acid (DHLA). Therefore, lipoic acid was reduced by tetrabutylammoniumborohydride (TBAB) in toluene in a molar ratio of 1:4 and added directly to the Ag NP solution. By adding the DHLA in toluene into the Ag NP solution, the dark brown particles started to agglomerate. This mixture was exposed to 336 nm UV light until the agglomerates stuck to the glass walls. After discarding the toluene, the Ag NCs could be dissolved in basic aqueous solution (pH 9). During this ligand exchange, the Ag NPs were etched down to a size of 2.2 ± 0.4 nm, and by replacing the DDAB by DHLA the resulting Ag NCs became water-soluble. Before using the Ag NCs, they were purified from bigger agglomerates and excess ligands first by gel electrophoresis and afterward by high performance liquid chromatography (HPLC). Additionally, the Ag NCs were characterized by UV−vis absorption, fluorescence spectroscopy, time-resolved photoluminescence (trPL), TEM, and dynamic light scattering (DLS).

■ ASSOCIATED CONTENT

Supporting Information

Synthetic and characterization details. Interaction of silver nanoclusters and cells. This material is available free of charge via the Internet at http://pubs.acs.org.

■ AUTHOR INFORMATION

Corresponding Author

*E-mail: wolfgang.parak@physik.uni-marburg.de (W.J.P.); jose.montenegromartos@physik.uni-marburg.de (J.M.M.M.).

Author Contributions

‖Both authors contributed equally to this study.

Notes

The authors declare no competing financial interest.

■ ACKNOWLEDGMENTS

This project has been funded by BMBF Germany (Project UMSICHT to W.J.P.) and NSC Taiwan (NSC 99-2120-M-038-001 and NSC 99-2911-I-033-003-2)

■ REFERENCES

(1) Zheng, J.; Nicovich, P. R.; Dickson, R. M. Highly Fluorescent Noble-Metal Quantum Dots. *Annu. Rev. Phys. Chem.* **2007**, *58*, 409−431.

(2) Lin, C. A. J.; Yang, T. Y.; Lee, C. H.; Huang, S. H.; Sperling, R. A.; Zanella, M.; Li, J. K.; Shen, J. L.; Wang, H. H.; Yeh, H. I.; Parak, W. J.; Chang, W. H. Synthesis, Characterization, and Bioconjugation of Fluorescent Gold Nanoclusters toward Biological Labeling Applications. *ACS Nano* **2009**, *3*, 395−401.

(3) Jin, R. Quantum sized, thiolate-protected gold nanoclusters. *Nanoscale* **2010**, *2*, 343−362.

(4) Scolari, M.; Mews, A.; Fu, N.; Myalitsin, A.; Assmus, T.; Balasubramanian, K.; Burghard, M.; Kern, K. Surface enhanced Raman scattering of carbon nanotubes decorated by individual fluorescent gold particles. *J. Phys. Chem. C* **2008**, *112*, 391−396.

(5) Wu, X.; He, X.; Wang, K.; Xie, C.; Zhou, B.; Qing, Z. Ultrasmall near-infrared gold nanoclusters for tumor fluorescence imaging in vivo. *Nanoscale* **2010**, *2*, 2244−2249.

(6) Lin, Y. H.; Tseng, W. L. Ultrasensitive sensing of Hg(2+) and CH(3)Hg(+) based on the fluorescence quenching of lysozyme type VI-stabilized gold nanoclusters. *Anal. Chem.* **2010**, *82*, 9194−9200.

(7) Xie, J.; Zheng, Y.; Ying, J. Y. Protein-directed synthesis of highly fluorescent gold nanoclusters. *J. Am. Ceram. Soc.* **2009**, *131*, 888−889.

(8) Whetten, R. L.; Khoury, J. T.; Alvarez, M. M.; Murthy, S.; Vezmar, I.; Wang, Z. L.; Stephens, P. W.; Cleveland, C. L.; Luedtke, W. D.; Landman, U. Nanocrystal gold molecules. *Adv. Mater.* **1996**, *8*, 428−433.

(9) Whetten, R. L.; Shafigullin, M. N.; Khoury, J. T.; Schaaff, T. G.; Vezmar, I.; Alvarez, M. M.; Wilkinson, A. Crystal Structures of Molecular Gold Nanocrystal Arrays. *Acc. Chem. Res.* **1999**, *32*, 397−406.

(10) Kawasaki, H.; Hamaguchi, K.; Osaka, I.; Arakawa, R. ph-Dependent Synthesis of Pepsin-Mediated Gold Nanoclusters with Blue Green and Red Fluorescent Emission. *Adv. Funct. Mater.* **2011**, *21*, 3508−3515.

(11) Liu, C. L.; Wu, H. T.; Hsiao, Y. H.; Lai, C. W.; Shih, C. W.; Peng, Y. K.; Tang, K. C.; Chang, H. W.; Chien, Y. C.; Hsiao, J. K.; Cheng, J. T.; Chou, P. T. Insulin-directed synthesis of fluorescent gold nanoclusters: preservation of insulin bioactivity and versatility in cell imaging. *Angew. Chem., Int. Ed.* **2011**, *50*, 7056−7060.

(12) Wang, H.-H.; Lin, C.-A. J.; Lee, C.-H.; Lin, Y.-C.; Tseng, Y.-M.; Hsieh, C.-L.; Chen, C.-H.; Tsai, C.-H.; Hsieh, C.-T.; Shen, J.-L.; Chan, W.-H.; Chang, W. H.; Yeh, H.-I. Fluorescent Gold Nanoclusters as a Biocompatible Marker for In Vitro and In Vivo Tracking of Endothelial Cells. *ACS Nano* **2011**, *5*, 4337−4344.

(13) Shang, L.; Azadfar, N.; Stockmar, F.; Send, W.; Trouillet, V.; Bruns, M.; Gerthsen, D.; Nienhaus, G. U. One-pot synthesis of near-infrared fluorescent gold clusters for cellular fluorescence lifetime imaging. *Small* **2011**, *7*, 2614−2620.

(14) Liu, H.; Zhang, X.; Wu, X.; Jiang, L.; Burda, C.; Zhu, J. J. Rapid sonochemical synthesis of highly luminescent non-toxic AuNCs and Au@AgNCs and Cu (II) sensing. *Chem. Commun.* **2011**, *47*, 4237−4239.

(15) Katzschmann, R.; Rehfeld, A.; Kranold, R. Optical anomaly of small particles in glasses. *Phys. Status Solidi A* **1977**, *40*, K161.

(16) Spanhel, L.; Haase, M.; Weller, H.; Henglein, A. Photochemistry of Colloidal Semiconductors. 20. Surface Modification and Stability of Strog Luminescing CdS Particles. *J. Am. Chem. Soc.* **1987**, *109*, 5649−5655.

(17) Bawendi, M. G.; Steigerwald, M. L.; Brus, L. E. The quantum mechanics of large semiconductor clusters ("quantum dots"). *Annu. Rev. Phys. Chem.* **1990**, *41*, 477−496.

(18) Ekimov, A. I.; Efros, A. L.; Onushchenko, A. A. Quantum size effect in semiconductor microcrystals. *Solid State Commun.* **1993**, *88*, 947−50.

(19) Alivisatos, A. P. Semiconductor Clusters, Nanocrystals, and Quantum Dots. *Science* **1996**, *271*, 933−937.

(20) Vosch, T.; Antoku, Y.; Hsiang, J.-C.; Richards, C. I.; Gonzalez, J. I.; Dickson, R. M. Strongly emissive individual DNA-encapsulated Ag nanoclusters as single-molecule fluorophores. *Proc. Natl. Acad. Sci. U.S.A.* **2007**, *104*, 12616−12621.

(21) Guo, C.; Irudayaraj, J. Fluorescent Ag Clusters via a Protein-Directed Approach as a Hg(II) Ion Sensor. *Anal. Chem.* **2011**, *83*, 2883−2889.

(22) Diez, I.; Pusa, M.; Kulmala, S.; Jiang, H.; Walther, A.; Goldmann, A. S.; Muller, A. H.; Ikkala, O.; Ras, R. H. Color tunability and electrochemiluminescence of silver nanoclusters. *Angew. Chem., Int. Ed.* **2009**, *48*, 2122−2125.

(23) Li, T.; Zhang, L.; Ai, J.; Dong, S.; Wang, E. Ion-Tuned DNA/Ag Fluorescent Nanoclusters As Versatile Logic Device. *ACS Nano* **2011**, *5*, 6334−6338.

(24) Le Guével, X.; Hötzer, B.; Jung, G.; Hollemeyer, K.; Trouillet, V.; Schneider, M. Formation of Fluorescent Metal (Au, Ag) Nanoclusters Capped in Bovine Serum Albumin Followed by Fluorescence and Spectroscopy. *J. Phys. Chem. C* **2011**, *115*, 10955−10963.

(25) Liu, S.; Lu, F.; Zhu, J. J. Highly fluorescent Ag nanoclusters: microwave-assisted green synthesis and Cr3+ sensing. *Chem. Commun.* **2011**, *47*, 2661−2263.

(26) Adhikari, B.; Banerjee, A. Facile Synthesis of Water-Soluble Fluorescent Silver Nanoclusters and HgII Sensing. *Chem. Mater.* **2010**, *22*, 4364−4371.

(27) Sharma, J.; Yeh, H.-C.; Yoo, H.; Werner, J. H.; Martinez, J. S. A complementary palette of fluorescent silver nanoclusters. *Chem. Commun.* **2010**, *46*, 3280−3282.

(28) Sharma, J.; Yeh, H. C.; Yoo, H.; Werner, J. H.; Martinez, J. S. Silver nanocluster aptamers: in situ generation of intrinsically fluorescent recognition ligands for protein detection. *Chem. Commun.* **2011**, *47*, 2294−2296.
(29) Yeh, H.-C.; Sharma, J.; Han, J. J.; Martinez, J. S.; Werner, J. H. A DNA-Silver Nanocluster Probe That Fluoresces upon Hybridization. *Nano Lett.* **2010**, *10*, 3106−3110.
(30) Yuan, X.; Luo, Z. T.; Zhang, Q. B.; Zhang, X. H.; Zheng, Y. G.; Lee, J. Y.; Xie, J. P. Synthesis of Highly Fluorescent Metal (Ag, Au, Pt, and Cu) Nanoclusters by Electrostatically Induced Reversible Phase Transfer. *ACS Nano* **2011**, *5*, 8800−8808.
(31) Shang, L.; Dong, S.; Nienhaus, G. U. Ultra-small fluorescent metal nanoclusters: Synthesis and biological applications. *Nano Today* **2011**, *6*, 401−418.
(32) Sperling, R. A.; Rivera_Gil, P.; Zhang, F.; Zanella, M.; Parak, W. J. Biological Applications of Gold Nanoparticles. *Chem. Soc. Rev.* **2008**, *37*, 1896−1908.
(33) Leuvering, J. H. W.; Thal, P. J. H. M.; Waart, M. v. d.; Schuurs, A. H. W. M. Sol Particle Agglutination Immunoassay For Human Chorionic-Gonadotropin. *Fresenius' J. Anal. Chem.* **1980**, *301*, 132.
(34) Elghanian, R.; Storhoff, J. J.; Mucic, R. C.; Letsinger, R. L.; Mirkin, C. A. Selective Colorimetric Detection of Polynucleotides Based on the Distance-Dependent Optical Properties of Gold Nanoparticles. *Science* **1997**, *277*, 1078−1081.
(35) Morones, J.; Elechiguerra, J.; Camacho, A.; Holt, K.; Kouri, J.; Ram, J.; Yacaman, M. The bactericidal effect of silver nanoparticles. *Nanotechnology* **2005**, *16*, 2346−2352.
(36) Baker, C.; Pradhan, A.; Pakstis, L.; Pochan, D. J.; Shah, S. I. Synthesis and antibacterial properties of silver nanoparticles. *J. Nanosci. Nanotechnol.* **2005**, *5*, 244−249.
(37) Sondi, I.; Salopek-Sondi, B. Silver nanoparticles as antimicrobial agent: a case study on E. coli as a model for Gram-negative bacteria. *J. Colloid Interface Sci.* **2004**, *275*, 177−182.
(38) Choi, O.; Deng, K. K.; Kim, N. J.; Ross, L. Jr.; Surampalli, R. Y.; Hu, Z. The inhibitory effects of silver nanoparticles, silver ions, and silver chloride colloids on microbial growth. *Water Res.* **2008**, *42*, 3066−3074.
(39) Fu, J.; Ji, J.; Fan, D.; Shen, J. Construction of antibacterial multilayer films containing nanosilver via layer-by-layer assembly of heparin and chitosan-silver ions complex. *J. Biomed. Mater. Res., Part A* **2006**, *79*, 665−674.
(40) Lok, C. N.; Ho, C. M.; Chen, R.; He, Q. Y.; Yu, W. Y.; Sun, H.; Tam, P. K.; Chiu, J. F.; Che, C. M. Proteomic analysis of the mode of antibacterial action of silver nanoparticles. *J. Proteome Res.* **2006**, *5*, 916−924.
(41) Gogoi, S. K.; Gopinath, P.; Paul, A.; Ramesh, A.; Ghosh, S. S.; Chattopadhyay, A. Green fluorescent protein-expressing Escherichia coli as a model system for investigating the antimicrobial activities of silver nanoparticles. *Langmuir* **2006**, *22*, 9322−9328.
(42) Rastogi, S. K.; Rutledge, V. J.; Gibson, C.; Newcombe, D. A.; Branen, J. R.; Branen, A. L. Ag colloids and Ag clusters over EDAPTMS-coated silica nanoparticles: synthesis, characterization, and antibacterial activity against Escherichia coli. *Nanomed. Nanotechnol. Biol. Med.* **2011**, *7*, 305−314.
(43) Tarantola, M.; Schneider, D.; Sunnick, E.; Adam, H.; Pierrat, S.; Rosman, C.; Breus, V.; Sonnichsen, C.; Basche, T.; Wegener, J.; Janshoff, A. Cytotoxicity of Metal and Semiconductor Nanoparticles Indicated by Cellular Micromotility. *ACS Nano* **2009**, *3*, 213−222.
(44) Eom, H.-J.; Choi, J. p38 MAPK Activation, DNA Damage, Cell Cycle Arrest and Apoptosis As Mechanisms of Toxicity of Silver Nanoparticles in Jurkat T Cells. *Environ. Sci. Technol.* **2010**, *44*, 8337−8342.
(45) Piao, M. J.; Kang, K. A.; Lee, I. K.; Kim, H. S.; Kim, S.; Choi, J. Y.; Choi, J.; Hyun, J. W. Silver nanoparticles induce oxidative cell damage in human liver cells through inhibition of reduced glutathione and induction of mitochondria-involved apoptosis. *Toxicol. Lett.* **2011**, *201*, 92−100.
(46) Díaz, B.; Sánchez-Espinel, C.; Arruebo, M.; Faro, J.; de Miguel, E.; Magadán, S.; Yagüe, C.; Fernández-Pacheco, R.; Ibarra, M. R.; Santamaría, J.; González-Fernández, Á. Assessing Methods for Blood Cell Cytotoxic Responses to Inorganic Nanoparticles and Nanoparticle Aggregates. *Small* **2008**, *4*, 2025−2034.
(47) Kittler, S.; Greulich, C.; Diendorf, J.; Koller, M.; Epple, M. Toxicity of Silver Nanoparticles Increases during Storage Because of Slow Dissolution under Release of Silver Ions. *Chem. Mater.* **2010**, *22*, 4548−4554.
(48) Li, P.-W.; Kuo, T.-H.; Chang, J.-H.; Yeh, J.-M.; Chan, W.-H. Induction of cytotoxicity and apoptosis in mouse blastocysts by silver nanoparticles. *Toxicol. Lett.* **2010**, *197*, 82−87.
(49) Diéz, I.; Ras, R. H. A. Fluorescent silver nanoclusters. *Nanoscale* **2011**, *3*, 1963−1970.
(50) Li, G.; Luo, Y.; Lu, W.; Li, J.; Jin, Y.; Guo, S. Dependence of Property of Silver Nanoparticles within Dendrimer-template on Molar Ratios of Ag+ to PAMAM Dendrimers. *Chin. J. Chem.* **2010**, *28*, 633−638.
(51) Gwinn, E. G.; O Neill, P.; Guerrero, A. J.; Bouwmeester, D.; Fygenson, D. K. Sequence-Dependent Fluorescence of DNA-Hosted Silver Nanoclusters. *Adv. Mater.* **2008**, *20*, 279−283.
(52) Cremer, G. D.; Antoku, Y.; Roeffaers, M. B. J.; Sliwa, M.; Noyen, J. V.; Smout, S.; Hofkens, J.; Vos, D. E. D.; Sels, B. F.; Vosch, T. Photoactivation of Silver-Exchanged Zeolite A. *Angew. Chem., Int. Ed.* **2008**, *47*, 2813−2816.
(53) Ozln, G. A.; Hugues, F.; Mattar, S. M.; McIntosh, D. F. Low Nuclearlty Sllver Clusters in Faujasite-Type Zeolites: Optical Spectroscopy, Photochemistry, and Relationship to the Photodlmerization of Alkanes. *J. Phys. Chem.* **1983**, *87*, 3445−3450.
(54) Zhang, H.; Huang, X.; Li, L.; Zhang, G.; Hussain, I.; Li, Z.; Tan, B. Photoreductive synthesis of water-soluble fluorescent metal nanoclusters. *Chem. Commun.* **2012**, *48*, 567−569.
(55) Shang, L.; Dong, S. Facile preparation of water-soluble fluorescent silver nanoclusters using a polyelectrolyte template. *Chem. Commun.* **2008**, 1088−90.
(56) Xu, H.; Suslick, K. S. Sonochemical Synthesis of Highly Fluorescent Ag Nanoclusters. *ACS Nano* **2010**, *6*, 3209−3214.
(57) Jana, N. R.; Peng, X. Single-phase and gram-scale routes toward nearly monodisperse Au and other noble metal nanocrystals. *J. Am. Chem. Soc.* **2003**, *125*, 14280−14281.
(58) Hull, S.; Keen, D. A. Pressure-induced phase transitions in AgCl, AgBr, and AgI. *Phys. Rev. B: Condens. Matter* **1999**, *59*, 750−761.
(59) Niggli, P. The crystal structure of several oxides. *Z. Kristallogr.* **1922**, *57*, 253−299.
(60) Sperling, R. A.; Liedl, T.; Duhr, S.; Kudera, S.; Zanella, M.; Lin, C.-A. J.; Chang, W.; Braun, D.; Parak, W. J. Size determination of (bio-) conjugated water-soluble colloidal nanoparticles - a comparison of different techniques. *J. Phys. Chem. C* **2007**, *111*, 11552−11559.
(61) Lakowicz, J. R. *Principles of Fluorescence Spectroscopy*; 3rd ed.; Springer: New York, 2006; p 954.
(62) Alvarez, M. M.; Khoury, J. T.; Schaaff, T. G.; Shafigullin, M. N.; Vezmar, I.; Whetten, R. L. Optical Absorption Spectra of Nanocrystal Gold Molecules. *J. Phys. Chem. B* **1997**, *101*, 3706−3712.
(63) Schaaff, T. G.; Shafigullin, M. N.; Khoury, J. T.; Vezmar, I.; Whetten, R. L.; Cullen, W. G.; First, P. N. Isolation of Smaller Nanocrystal Au Molecules: Robust Quantum Effects in Optical Spectra. *J. Phys. Chem. B* **1997**, *101*, 7885−7891.
(64) de Heer, W. A. The physics of simple metal Clusters: experimantal aspects and simple models. *Rev. Mod. Phys.* **1993**, *65*, 611−676.
(65) Schaaff, T. G.; Knight, G.; Shafigullin, M. N.; Borkman, R. F.; Whetten, R. L. Isolation and Selected Properties of a 10.4 kDa Gold: Glutathione Cluster Compound. *J. Phys. Chem. B* **1998**, *102*, 10643−10646.